

Evaluation of Progressive Failure of Composite T-Joint Using Mixed Mode Cohesive Zone Model

A. Sane¹ · D. R. Peshwe² · C. M. Manjunatha³ · P. M. Padole¹ · R. V. Uddanwadiker¹

Received: 25 January 2017 / Accepted: 21 August 2017 / Published online: 11 September 2017
© The Indian Institute of Metals - IIM 2017

Abstract T shaped stiffeners are the most commonly used structures in aerospace components. De-lamination/de-bond initiation followed by its growth is one of the most common reasons for failure in a fiber reinforced composite structure. It is caused by the interlaminar normal and shear stresses between different structural constituents. In a typical structural T-joint, the failure mechanism and location may differ based on the structural design parameters like fillet radius, thickness, layup sequence, filler stiffness, etc. In this study, finite element analysis has been performed using cohesive zone model (CZM) on a composite T-joint to simulate the pull out test conditions. A simplified plane strain model coupled with CZM is proposed, which can evaluate the failure initiation and progression accurately with lesser computational efforts. The final failure occurs at a displacement of 8.04 mm and the computed failure load is 2240 N. The results obtained by the proposed numerical model are validated by experimental results and it is observed that predicted regions of failure, failure displacements and failure load calculated are correlating reasonably well with the experiment.

Keywords Carbon fiber composite · FE analysis · T-joint · Cohesive zone modeling

1 Introduction

One of the most common design in aerospace structures is the T shaped stiffened joints consisting of a thin laminate skin reinforced with a T section laminate stiffener, which is joined to the skin by co-curing or adhesive bonding. The use of bonding methods has increased recently because of the benefits of reducing the number of parts in a structure.

Many researchers have earlier worked in the area of failure study of sandwich T Joints. Guo [1] investigated the failure mechanism and alternative design for composite sandwich T-joints subjected to tensile load for assessing their strength. A finite element model to analyze the structural deformation, strength and delamination fracture of composite T joints which are reinforced using z-pins was proposed by Bianchi [2]. Experimental results for carbon/epoxy z-pin reinforced composite T-joints tested in pull-off loading was presented by Park [3]. Static structural response of a composite T joint containing a viscoelastic insert was investigated by numerical method and FEM by Blake [4]. Da Silva [5] presented analytical and experimental results for finding strength of adhesively bonded T-joints with a range of reinforcing methods.

The cohesive zone modeling technique were also used by some of the researchers to analyze composite joints. Khalili [6] analyzed the effect of fillet geometry and core material of sandwich panels on the performance of T-joints by numerical analysis. An experimental and analytical study into the importance of the skin–flange thickness on the strengthening mechanics and fracture modes of Z pinned composite T-joints was presented by Koh [7]. Alfano [8] dealt with the application of cohesive zone model to study mode I fracture in adhesively bonded joints. However these studies have considered only one of the parameters such as fillet geometry, core material, interface

✉ D. R. Peshwe
peshwedilip1@gmail.com

¹ Department of Mechanical Engineering, Visvesvaraya National Institute of Technology, Nagpur, India

² Department of Metallurgical and Materials Science Engineering, Visvesvaraya National Institute of Technology, Nagpur, India

³ Fatigue and Structural Integrity Group, Structural Technologies Division, CSIR-NAL, Bangalore, India

reinforcement techniques and its effect on failure behavior of the joint considering only one mode of failure at a time.

Various researchers have done experimental analysis on the T connections of different configurations. It has been observed that the most likely zone of failure in a T joint is near the filler area. Davies [9] reported that debond failure are at interface of filler and composite layer. Debond between stringer plies at fillet area was reported by Meeks [10]. Orifici [11] reported failure at the tip of the stiffener.

It is observed that the researchers have either used the experimental techniques or analytical models to study failure under pure mode I or mode II fracture criteria. However it has been observed that the failure in joints occur due to the combined effect of mode I and mode II fracture energies and it is dependent on a single variable G_C which is a function of G_{Ic} , G_{IIc} and G_T ($G_{Ic} + G_{IIc}$).

The literature survey indicates that researchers so far haven't studied the failure of joints under mixed mode loading while using the plane strain approach coupled with mixed mode CZM and scalar degradation of material. The objective of the current study is to investigate the fracture behavior of a composite T-joint using a simplified approach. A mixed mode CZM based FE model for an adhesively bonded composite T-joint is considered for analysis using Abaqus. The problem is assumed as a generalized plane strain problem and it also considers the degradation of mechanical properties of the adhesive at the interface.

2 FE Modeling

2.1 Cohesive Zone Model

Cohesive zone model is one of the most popular techniques for analyzing the fracture of structures. It's being used over the conventional techniques like virtual crack closure technique (VCCT) because it can capture both the damage nucleation and evolution. It considers the fracture formation as a gradual event, in which the separation of the surfaces take place across some predefined crack paths or cohesive zones and is resisted by cohesive tractions.

The Mode I dominated bilinear CZM model proposed by Alfano [12] assumes that the separation of the material interfaces is dominated by the displacement jump normal to the interface as shown in Fig. 1. The area under the curve is the energy released due to debonding and is called the critical fracture energy. The relation between normal cohesive traction t_n and normal displacement jump δ_n can be expressed as

$$T_n = K_n \delta_n (1 - D_n) \quad (1)$$

where;

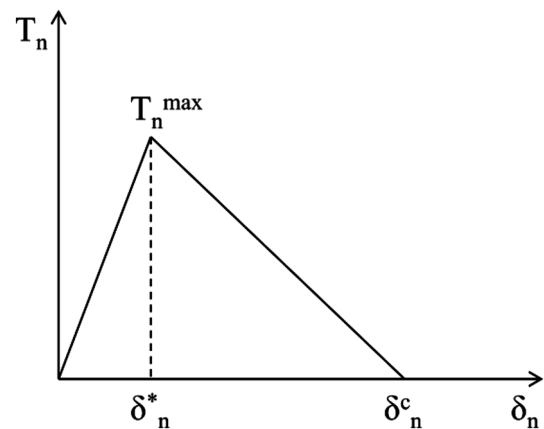


Fig. 1 Traction separation curve under normal loading

$$K_n = \text{Normal cohesive stiffness} = \frac{T_n^{\max}}{\delta_n^*},$$

$D_n = \text{Damage parameter (varies from 0 to 1)}$.

The Mode II dominated bilinear CZM model assumes that the separation of the material interfaces is dominated by the displacement jump that is tangent to the interface, as shown in Fig. 2. The relation between tangential cohesive traction t_t and tangential displacement jump δ_t can be expressed as:

$$T_t = K_t \delta_t (1 - D_t) \quad (2)$$

where;

$$K_t = \text{Tangential cohesive stiffness} = \frac{T_t^{\max}}{\delta_t^*},$$

$D_t = \text{Damage parameter (varies from 0 to 1)}$.

For bilinear cohesive law under the mixed-mode fracture, the separation of material interfaces depends on normal as well as tangential components of traction. To predict the damage nucleation correctly, the interaction between these two traction components has been modeled

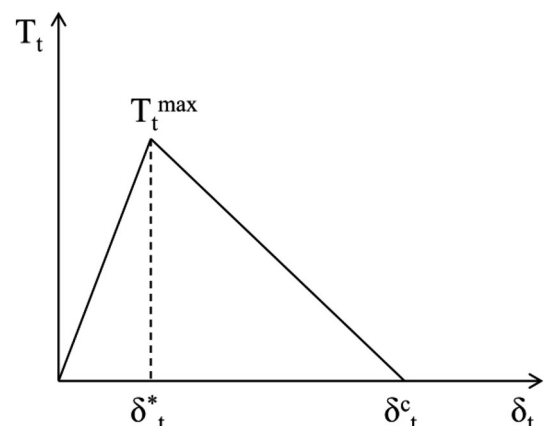


Fig. 2 Traction separation curve under shear loading

using the quadratic stress criterion. This criteria is a function of normal and shear components of traction and expressed as shown in Eq. 3.

$$\left(\frac{t_n}{t_{I0}}\right)^2 + \left(\frac{t_t}{t_{II0}}\right)^2 + \left(\frac{t_s}{t_{III0}}\right)^2 = 1 \tag{3}$$

where t_n , t_t , and t_s are stresses in normal and two shear directions respectively and t_{I0} , t_{II0} and t_{III0} are critical values of stresses in normal and two shear directions.

When the damage initiation criterion is fulfilled, the cohesive stiffness degrades at a rate based on the damage evolution model. A scalar damage parameter D is introduced which increases monotonically from 0 to 1 when the loading is increased.

The mixed-mode criterion proposed by Benzeggagh and Kenane [14] is used (B–K criterion) to accurately predict the final failure. This criterion is expressed as a function of the Mode I and Mode II fracture toughness values

$$G_{IC} + (G_{IIC} - G_{IC}) \left(\frac{G_{II}}{G_T}\right)^\eta = G_C \tag{4}$$

where,

$$G_T = G_{Ic} + G_{IIc}.$$

The value of the exponent η is taken from the interface properties as given in Table 3.

2.2 Specimen and Materials

The specimen configuration considered in this investigation is shown schematically in Fig. 3. It consists of four components namely the skin, filler and left & right stringer legs. The skin thickness of 1.2 mm, stringer leg thickness of 0.9 mm and ply thickness of 0.15 mm is used for modeling. The adhesive layers run along the inner surface of each of the stiffener legs and skin filler interface.

Table 1 show the layup sequence used in different section of the joint.

The IM7/8552 composite material is used as lamina material and the components are joined together using

FM300 adhesive. Tables 2 and 3 shows the material properties and interface properties of IM7/8552 UD composite lamina and FM300 adhesive, where t_{I0} , t_{II0} , t_{III0} are interlaminar strengths and G_{IC} , G_{IIC} , G_{IIIC} are critical strain energy release rates.

2.3 Modeling of T-Joint

In the first stage, all the four components of the joint have been modeled and material properties, layer stacking sequence etc. are assigned. In the second stage, the adhesive layer between the skin-stiffener interfaces and in the Bermuda triangle or resin filled areas have been modeled.

Local coordinate systems are created for defining material orientation in different areas. The areas have been meshed using CPE4/CPE3 plain strain elements using a structured quad dominated mesh. This ensures minimum distortion of the elements at the sharp corners of the resin rich region. The element sizing is done in such a way that there are two rows of elements in each layer so that the results can be calculated at the mid-plane of each layer. For defining the cohesive interaction between the four sections, two dimensional cohesive element COH2D4 is selected. A node to surface contact is established between the sections which is numerically more efficient. Figure 4 shows the meshed model of configuration.

For better establishment of contact pairs, small node adjustments are allowed. In order to accurately predict the failure, the mixed-mode criterion proposed by Benzeggagh and Kenane [14] (B–K criterion) is used. This criterion is expressed as a function of the Mode I and Mode II fracture toughness of the material and a parameter obtained from mixed mode bending tests at different mode ratios.

A displacement boundary condition is applied in incremental steps on the stiffener to calculate reaction load and the ends of the skin are fixed in both X and Y direction. The model thus created is solved for a non-linear analysis.

Fig. 3 Schematic of T-Joint studied

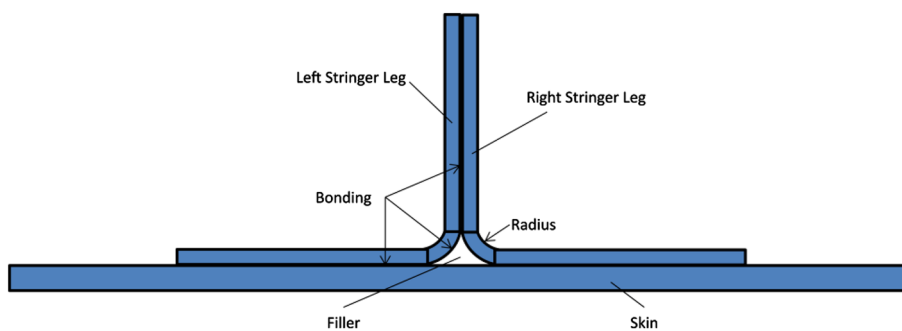


Table 1 Layup sequences

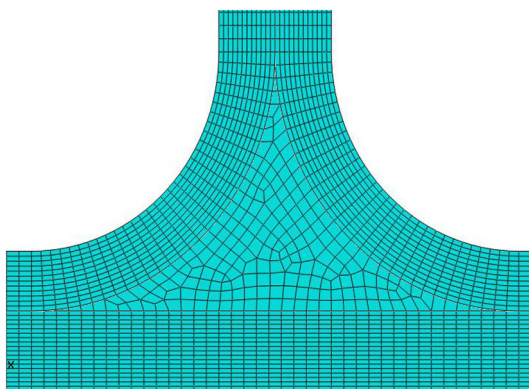
Section	Layup
Skin	[45 ₂ /0/90/90/0/45 ₂]
Left stringer leg	[45 ₂ /0 ₂ /90 ₂]
Right stringer leg	[45 ₂ /0 ₂ /90 ₂]

Table 2 Material properties

IM7/8552 UD composite lamina					
E ₁	147 GPa	ν ₁₂	0.3	G ₁₂	6 GPa
E ₂	11.8 GPa	ν ₂₃	0.3	G ₂₃	6 GPa
E ₃	11.8 GPa	ν ₁₃	0.475	G ₁₃	6 GPa
Adhesive FM300					
E	2.38 GPa	ν	0.38	G	0.86 GPa

Table 3 Interface properties [11, 13]

	IM7/8552	FM300
t ₁₀ (MPa)	50	60
t ₁₁₀ (MPa)	100	90
t ₁₁₁₀ (MPa)	100	90
G _{IC} (N/mm)	0.9	0.24
G _{IIc} (N/mm)	2.5	0.5
G _{IIIc} (N/mm)	2.5	0.5
η	8	4.6

**Fig. 4** Meshed model of joint

3 FE Analysis Results

Finite element analysis is carried out to obtain load displacement relationship for the T joint using mixed mode cohesive zone model and it is compared with the experimental data as shown in Fig. 5. From the load displacement

curve, it is clear that the initial de-bond occurs at a displacement of 6.91 mm, due to which the overall stiffness of the joint reduces and there is a load drop in the curve. The load then increases further and final failure occurs at a displacement of 8.04 mm.

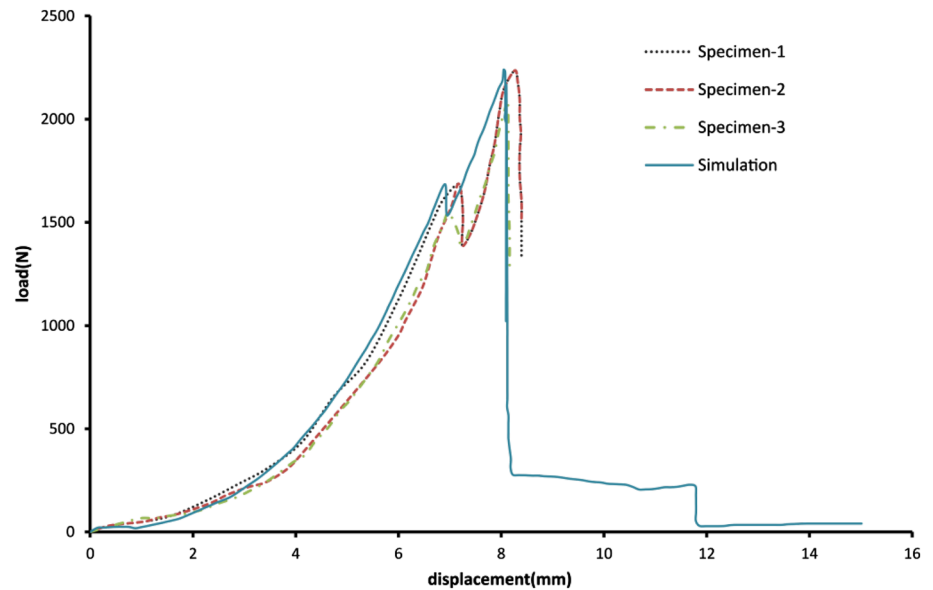
It has been shown in the past that sometimes the results of FE analysis tend to vary when the mesh size of the model is changed. This happens especially in cases where geometric/material nonlinearities are involved. To check the effect of mesh refinement on the cohesive model, a sensitivity analysis has also been carried out. The element size for the skin and stringer legs changes to 0.1 mm and three elements are taken along thickness direction for each ply. For the cohesive layers, an element size of 0.05 mm is selected and filler is meshed with an element size of 0.2 mm.

It is observed that convergence difficulties occur after the refinement of the mesh. To overcome this issue, small time increments are selected. The comparative load displacement curves of the coarse and fine mesh are found to be almost the same. The behavior of model in terms of failure location and failure load remains the same. The disadvantage of the finer mesh is longer computational time.

It is observed that stress concentration occurs at the filler tip and filler-composite interfaces at a corresponding displacement of 6.60 mm (just before crack initiation). Debonding initiates at the filler composite interface of the joint for a corresponding displacement of 6.91 mm. A similar behavior is observed in the experimental study as well. The final failure is observed at a displacement of 8.04 mm and corresponding load of 2240 N. The adhesive bonds at skin-stringer, left-right stringer legs and stringer leg-resin are found to fail, and delamination is observed in skin plies. The results obtained from the numerical analysis are in congruence with the experimental findings; however the simulation results are a little stiffer than the test data.

4 Experimental Observation

The T-joint considered in this study is made up of IM7/8552 UD composite lamina and assembled together using FM300 film adhesive. The joint contain four sections out of which three are made up of composite lamina and the delta region is filled with epoxy filler. A test fixture is designed and fabricated for the pull out test. The test fixture with the specimen is placed onto the machine for pull out test. A ramp rate of 0.5 mm/min is employed for the tensile test and load displacement data is generated for three specimens as shown in Fig. 5. There is a very minor variation in the load-displacement curves obtained from each specimen, also the location of failure remains similar for all

Fig. 5 Experimental and FE load–displacement curves

specimens as shown in Fig. 5. Experimentally it is observed that debonding starts at the tip of the nodule region and the crack grows towards the skin-stiffener and left–right stringer leg interfaces with subsequent increase in load. The final failure occurs at a load of 2240 N with a corresponding displacement of 8.04 mm.

Figure 6a shows the T-joint and the test fixture on the servo hydraulic UTM. Figure 6b shows the initiation of debond at the tip of the filler. Figure 6c shows the evolution of debond at multiple composite-filler interfaces when loaded further. FE analysis results are presented in Fig. 6d–f. Figure 6d shows the deformed joint just before the initiation of crack, Fig. 6e shows the initiation of failure at one of the interfaces and Fig. 6f shows the final de bonded structure. The simulation results correlates well with the experimental observations.

5 Discussion

From the load displacement curve, it is clear that the initial de-bond occurs at a displacement of 6.91 mm, due to which the overall stiffness of the joint reduces and there is a load drop in the curve. The load then increases further and final failure occurs at a displacement of 8.04 mm which is similar to the experiment. From fig 5, it can also be concluded that the mechanical property degradation incorporated in the CZM based model works quite well and the stiffness of the joint keeps changing with every load step. It is clear from the load–displacement curve that the stiffness of the joint keeps on increasing until the point of first measurable debond. At this point, the stiffness is

230.92 N/mm. After the initiation of this debonds, the stiffness drops to 209.73 N/mm which is 9% less than the stiffness at the point of debond.

The normal and shear stress contour in the joint at a displacement of 6.60 mm which is just before the initial debond indicates that the filler tip and filler-composite interfaces are the stress concentration locations. The normal stress component S22 is highest at the tip of the filler area and the shear stress component S12 attains its highest value at the filler tip interface. Until this point of time there is no crack in the structure and is still in the elastic phase. The stress concentration at the filler tip and filler composite interface indicates that these are the most likely locations of crack nucleation.

The initial debond occurs at a displacement of 6.91 mm and corresponding load is 1684 N. Experimentally also the debond initiates at displacement of 6.96 mm and the calculated load is 1609 N. Debonding starts at the filler composite interface in the joint. At the initial debond, there is a load drop in both the FE and experimental load displacement curves as shown in Fig. 5.

Debonds are predicted at the filler-stringer leg, left–right stringer legs and stringer legs-skin interfaces through simulation and delamination is recorded in plies of skin. The T-joint fails at a displacement of 8.04 mm with corresponding load of 2240 N which is in good correlation with the experimental failure displacement of 8.02 mm with corresponding load of 2167 N. The experimental observations made by Davies [9] and Meeks [10] show that in most of the cases, debonding occurs at interface and debonding at stiffener which in turn confirms the correctness of the results in the current study. The sensitivity analysis indicates that the proposed model is numerically

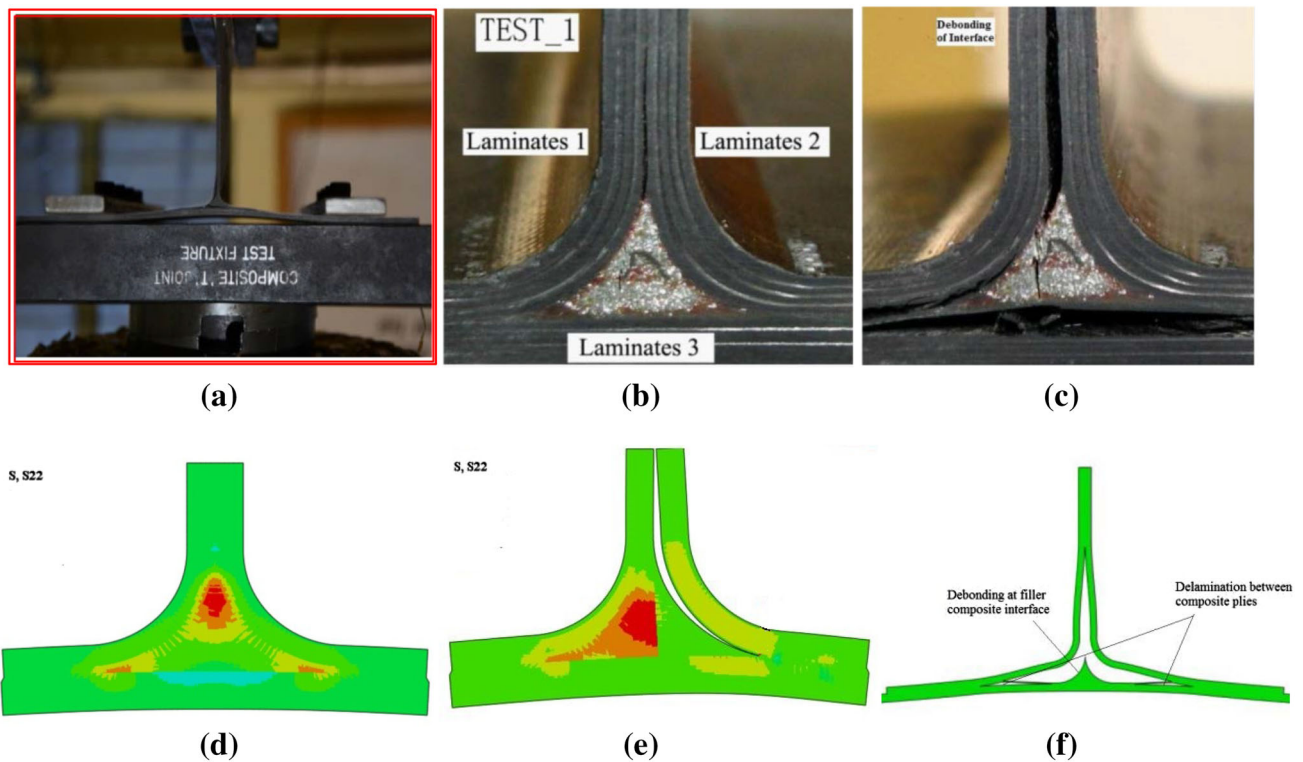


Fig. 6 Experimental and FE results for crack initiation and propagation

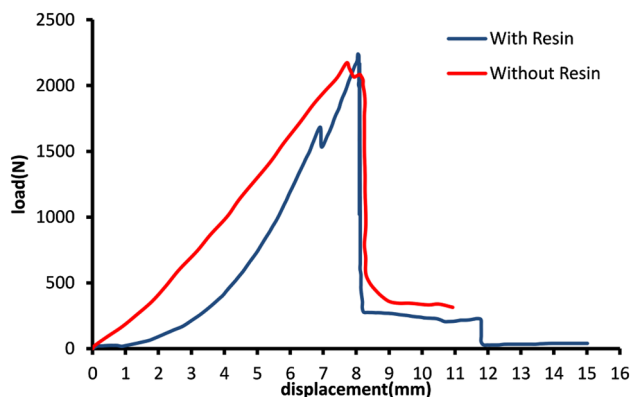


Fig. 7 Comparative load–displacement curves (with and without resin)

stable and the results of simulation doesn't change when the mesh is refined.

A parametric study is performed to find out that, how the filler resin affect the load bearing capacity of joint. The filler resin section and the contact interfaces associated with it are deleted from the joint assembly. The simulation is performed on model consisting of baseplate and two stinger legs. Figure 7 shows the comparison of the models with and without resin.

The joint without resin exhibits a linear load displacement relationship throughout the loadstep, than the joint with resin. It is also observed that there is no intermediate

load drop. When compared with the joint with resin, it is observed that the load bearing capacity slightly reduces to 2171.83 N (2240 N with resin) and the corresponding displacement is 7.7 mm (8.04 mm with resin).

6 Conclusions

This study based on cohesive zone model predicts the failure behavior of the skin stringer interface accurately. The damage initiation criteria based on maximum traction values is able to predict the initial debond at the interfaces. The damage evolution criteria based on energy release rates calculates the scalar degradation of material after initial debond and employ the decreased stiffness values to evaluate final failure. In the present FE study, a decrease in stiffness of about 9% is observed after the first debond which is in good agreement with the experimental observation. The debonding failure initiates at a displacement of 6.91 mm; followed by this, the overall stiffness of the joint reduces. The failure further progresses and final failure occurs at a displacement of 8.04 mm and a load of 2240 N with multiple debonds. The predicted regions of failure match with the experimental study performed and previous studies on the T-joints of simple configuration. When the joint is simulated without resin in the nodule region, results exhibit a linear load displacement relationship with failure

displacement of 7.7 mm and failure load of 2171.83 N. Sensitivity analysis indicates that the mesh refinement doesn't change the analysis results in terms of failure location/load and confirms an acceptable level of accuracy of the FE model. The plane strain model coupled with CZM is able to predict the failure initiation and growth of simple configurations precisely with a fairly lesser computational effort.

References

1. Guo S, and Morishima R, *Compos Struct* **94** (2011) 229.
2. Bianchi F, *Compos Sci Technol* **73** (2012) 48.
3. Park Y-B, *Compos Struct* **94** (2012) 625.
4. Blake J I R, *Compos Part A* **32** (2001) 641.
5. Da Silva L F M, and Adams R D, *Int J Adhes Adhes* **22** (2002) 311.
6. Khalili S M R, and Ghaznavi A, *Int J Adhes Adhes* **31** (2011) 347.
7. Koh T M, Feih S, and Mouritz A P, *Compos Part A* **43** (2012) 1308.
8. Alfano M, *Key Eng Mater* **348–349** (2007) 13.
9. Davies G A O, and Ankersen, J, *J Mater Sci* **43** (2008) 6586.
10. Meeks, C, Greenhalgh E, and Falzon B G, *Compos Part A* **36** (2005) 934.
11. Orifici A C, Thomson R S, Degenhardt R, Bisagni C, and Bayandor J, *J Compos Mater* **43** (2009) 3239.
12. Alfano G, and Crisfield M A, *Int J Numer Methods Eng* **50** (2001) 1701.
13. Psarras S, Pinho S T, and Falzon B G, *Damage-Tolerant Design of Stiffener Run-Outs: A Finite Element Approach*, InTech (2012).
14. Benzeggagh M K, and Kenane M, *Compos Sci Technol* **56** (1996), 439.